PLOS GENETICS

IgH 3' regulatory region increases ectopic class switch recombination

Sandrine Le Noir[1]*, **Amélie Bonaud**[1¤], **Bastien Hervé**[2], **Audrey Baylet**[1], **François Boyer**[1], **Sandrine Lecardeur**[1], **Zeliha Oruc**[1], **Christophe Sirac**[1], **Michel Cogné**[1,3]*

1 UMR CNRS 7276, INSERM 1262 and Université de Limoges: Contrôle de la Réponse Immune B et Lymphoprolifération, 2 rue du Pr. Descottes, Limoges, France, **2** Université de Limoges, US 42/UMS2015 plateforme Biologie Intégrative Santé Chimie Environnement (BISCEm), Limoges, France, **3** Institut Universitaire de France, Paris, France

¤ Current address: Team "Chemokine regulated interplays between lymphocytes and their environment"Inserm U1160 "EMiLy". Institut de Recherche Saint-Louis 1 avenue Claude Vellefaux Paris, France
* sandrine.le-noir@unilim.fr(SLN); michel.cogne@unilim.fr(MC)

Abstract

DNA lesions inflicted by activation-induced deaminase (AID) instrumentally initiate the processes reshaping immunoglobulin genes in mature B-cells, from local somatic hypermutation (SHM) to junctions of distant breaks during class switch recombination (CSR). It remains incompletely understood how these divergent outcomes of AID attacks are differentially and temporally focused, with CSR strictly occurring in the Ig heavy chain (*IgH*) locus while SHM concentrates on rearranged V(D)J regions in the *IgH* and Ig light chain loci. In the *IgH* locus, disruption of either the 3'Regulatory Region (3'RR) super-enhancer or of switch (S) regions preceding constant genes, profoundly affects CSR. Reciprocally, we now examined if these elements are sufficient to induce CSR in a synthetic locus based on the *Igκ* locus backbone. Addition of a surrogate "core 3'RR" (c3'RR) and of a pair of transcribed and spliced Switch regions, together with a reporter system for "κ-CSR" yielded a switchable *Igκ* locus. While the c3'RR stimulated SHM at S regions, it also lowered the local SHM threshold necessary for switch recombination to occur. The 3'RR thus both helps recruit AID to initiate DNA lesions, but then also promotes their resolution through long-distance synapses and recombination following double-strand breaks.

Author summary

Class switching allows B lymphocytes to replace expression of immunoglobin M with that of immunoglobulins G, A or E. The genetic support of class switching, is a unique and large deletion uniquely occuring within the immunoglobulin heavy chain (IgH) locus. This recombination is triggered after DNA lesions inflicted by the activation-induced deaminase (AID) enzyme. In immunoglobulin light chain loci, AID only stimulates somatic hypermutation. In such a non-IgH locus, we now show that the IgH 3' superenhancer can promote junctions between distant DNA breaks and ectopic class switch

recombination. This study identifies the minimal elements necessary for class-switch
recombination to occur instead of hypermutation in a locus targeted by AID, *i.e.* tran-
scribed (and spliced) target sites for AID in so-called S regions, and the 3'IgH superenhan-
cer which both helps recruit AID for DNA lesions, and helps repair these lesions through
distant gene synapsis and recombination.

Introduction

The Activation-Induced Deaminase (AID) enzyme has multiple roles in the B-cell lineage and
their differential regulation remains to be fully characterized. In all species synthesizing Ig,
AID primarily provides Ig variable (V) gene diversification through SHM or gene conversion
(GCV) [1]. This ancestral repertoire broadening is even shared with an AID ortholog for the
lamprey antigen receptors [2]. In frogs, birds and mammals, evolution endowed AID with the
additional role to initiate CSR after DNA lesions affecting target S regions upstream of *IgH*
constant (C_H) genes [3].

In mouse B-cells, the 3'Regulatory Region super-enhancer (3'RR) is the master *cis*-regula-
tory element controlling the activities of AID within the *IgH* locus, either for SHM, CSR or
locus suicide recombination (LSR) [4–7]. SHM and CSR follow B-cell activation. AID lesions
in S regions initiate some low-level local SHM but more dramatically yield DNA double strand
breaks (DSBs), followed by junctions at long distances [8]. The 3'RR modulates germline tran-
scription of C_H genes in activated B-cells, chromatin remodeling of S regions and AID recruit-
ment to acceptor S regions [9]. Mammalian S regions consist of 1–10 kb-long highly repetitive
G-rich DNA sequences containing clustered RGYW AID consensus motifs [10]. The mouse
3'RR includes 4 core enhancers: *hs3a*, *hs1,2*, *hs3b* and *hs4*. In addition to binding specific tran-
scription factors, enhancers included in the 3'RR are transcribed into eRNA [7], and their
function is regulated by a distantly transcribed long non-coding RNA (lncRNA) [11]. The first
three enhancers are embedded within a ~25-kb dyad symmetry, while the fourth stands down-
stream [12, 13]. The four core enhancers combined into a short (2.1 kb) "core 3'RR" (c3'RR)
show strong synergy and transcriptional activity, although not reaching that of the complete
30kb-long full-length *3'RR* [13].

The specific contribution of the *3'RR* in SHM, DNA breakage and joining of broken S
regions remains elusive, since multiple knock-out experiments (KO) in the *IgH* locus all
showed global defects and failed to uncouple the 3'RR functions in transcription or initiation
of SHM and CSR [14]. While the 3'RR clearly promotes SHM and carries at least a dual role
regarding both SHM and CSR, its influence on CSR is the best documented and most critical
in the *IgH* locus. It is necessary for optimal germline transcription of acceptor S regions and its
deletion almost abrogates accessibility of these S regions while preserving some accessibility to
Sμ [4–6, 15]. S regions from 3'RR-deficient B-cells also show a loss of the chromatin marks
H3K9ac and H3K4me3, for which they are normally enriched prior to CSR in activated B-cells
[15–18]. Finally, the 3'RR likely helps synapsis of broken S regions, then defining chromo-
somal loops between S regions that stand on the same allele [19].

While the 3'RR helps recruit AID, it thus clearly mediates additional effects that are impor-
tant for CSR. An ideal way to evaluate those additional effects is to introduce the c3'RR into a
locus that efficiently recruits AID beforehand for SHM.

In a previously developed model of ectopic CSR, a complete CSR substrate was designed,
providing all the S sequences, transcription and splicing patterns known to be important for
local recruitment of AID [20]. This substrate was introduced into the *Igκ* "*KIKS*" locus and

underwent high transcription accompanied by efficient SHM and presence of localized internal S region deletions (ISD) [20]. Despite this efficient targeting by AID, "κ-CSR" events joining a pair of ectopic S regions remained exceptional and clearly much rarer than for "IgH-CSR", with a defect likely affecting the occurrence of synapses between distant AID targets [20].

We hypothesized that these ectopic S regions inserted into an *Igκ* location exposed to AID, would provide an ideal model to explore the role of the 3'RR beyond AID recruitment and check whether this super-enhancer could be the missing piece of an *Igκ* switchable locus. We thus tried complementing the *KIKS* CSR substrate with a core "c3'RR" cassette, in order to facilitate tethering of two distant κ-S regions and check whether this could raise the level of κ-CSR closer to that of classical IgH-CSR.

Material and methods

Ethics statement

Procedures were reviewed and approved by the Ministère de l'Education Nationale de l'Enseignement Supérieur et Recherche autorisation APAFIS#16151-2018071716292105v3.

Mice

The strategy used to generate *c3'RR-KIKS* mice was identical to that previously described for *KIKS* mice [20], except for the inclusion of a c3'RR cassette downstream of the genomic fragment containing the *Eiκ* enhancer and *Cκ* gene. The *c3'RR* cassette included all four *3'RR* enhancers in their normal palindromic layout, as described [13]. Knock-in was done in CK35 embryonic stem cells, which were injected into blastocysts. After germline transmission, mice were bred with a *cre*-expressing strain to delete the Neo^R cassette. *KIKS*, *c3'RR-KIKS* and *c3'RR-KIKS* / *Aicda$^{-/-}$* mice were used. All animal strains were bred and maintained in SOPF conditions.

ELISA assays

ELISAs for the presence of murine and human Igκ were performed on serum from *KIKS*, *c3'RR-KIKS* and *c3'RR-KIKS* / *Aicda$^{-/-}$* as described [20].

Flow cytometry and cell sorting

Antibodies used for staining and sorting are detailed in S1 Table. Flow cytometry analyses were done on a BD Pharmingen LSRFortessa cytometer. Data were then analyzed with BD FACSDiva software (BD Biosciences, San Jose, CA). Gating strategy is shown in S2 Fig. Sorting was performed on a FACS ARIA 3 (BD Biosciences).

Immunization

Groups of 8-week-old mice were immunized by intraperitoneal injection of 200 µl SRBC and analyzed 8 days later.

SHM and switch junction analyses

SHM and switch junction analyses were performed on B220$^+$/GL7$^+$ and B220$^+$/Igκ$^+$ cells from Peyer's patches, respectively, using previously described primers for *Jκ5* 3' flanking intron and switch junction [20] and LVk4-63F: 5'- TGC AGA TTT TCA GCT TCC TG-3' and Sγ3R: 5'- CCT CAC CCA CCC TAG CTC A-3' for κ-Sγ3 region. PCR products (100ng) were

fragmented using Ion Shear Plus reagents kit (Life Technologies), then barcodes and adaptors were ligated using Ion Xpress Plus Fragment (Life Technologies). Fragments around 200pb were selected using E-Gel Size Select 2% (Life Technologies) and sequenced on an Ion Proton System. Raw files were generated using Ion Torrent Suite (adapter- and barcode-trimmed), and junctions were analyzed using CSReport, together with mutation frequency [21]. Mutation frequency was analyzed using DeMinEr tool [22]. Sequences are deposited under the reference PRJEB34851.

Transcript analysis

Total RNA from Peyer's patches was extracted with TRI Reagent (Ambion, Austin, TX), and 1 μg was used for cDNA synthesis using random primers (Applied Biosystems). Relative quantification of primary transcripts was performed with SYBR green Master Mix (Applied Biosystems) by reference to GADPH levels. QPCR primers and assays were as previously described [20].

Cell culture

Splenocytes were collected, red blood cells were lysed and cells were CD43-depleted using CD43 microbeads (Miltenyi Biotec). Splenic B lymphocytes were cultured for 3 days in RPMI containing 10% FCS with LPS (1μg/mL, B4 Invivogen) or LPS + IL4 (20ng/mL, Peprotech). Cells and supernatants were recovered for LAM-HTGTS experiments and ELISA.

LAM-HTGTS

LAM-HTGTS was performed as previously described [23] using activated splenocytes or Peyer's patches cells (enriched with the STEMCELL "B-cell isolation kit"). Jκ5-biotin (5'-TGT GTA AGA CAC AGG TTT TCA TGT) and Jκ5-nested (5'- CAG AAA ATC TTG AGA AAA TGG AGA-3') primers and Sμ primers [24] were used to generate libraries. Data analysis of MiSeq sequencing reads was performed as previously described [25]. Graphical representation were performed as previously described [26]. All sequence alignments were done with the mouse mm10 genome (or its variant sequence corrected for our *KIKS* changes to the *Igκ* locus (Figs 1 and S1). Sequences are deposited under the reference PRJEB34781.

Statistical analysis

Statistical tests used in the study are indicated in the figure legends and performed using GraphPad Prism (*p<0.05, **p<0.01, ***p<0.001, ****p<0.0001).

Results and discussion

c3'RR-KIKS locus description and B-cell development

To determine whether the *3'RR* super-enhancer could by itself affect the output of AID-initiated single nucleotide lesions and increase the balance of distant recombination *vs* local alteration, we studied *Igκ* loci modified in order to support ectopic CSR. The *KIKS Igκ* variant locus (carrying only paired S regions) is known to show low-levels of κ-CSR junctions after AID-mediated DNA lesions [20]. We compared it to a *c3'RR-KIKS* variant carrying not only an κ-*Sμ*/κ-*Sγ3* pair but also a surrogate *c3'RR* super-enhancer cassette (Figs 1A and S1). The *c3'RR* included the four core enhancers (*hs3a*, *hs1.2*, *hs3a* and *hs4*) of the *IgH 3'RR*. We have previously described that the insertion at the *Igκ* locus in the *KIKS* mice does not disturb early and late B cell development compared to *wt* mice. For this reason we only compared the two KI mouse models [20]. Normal early B-cell development occurred in both homozygous
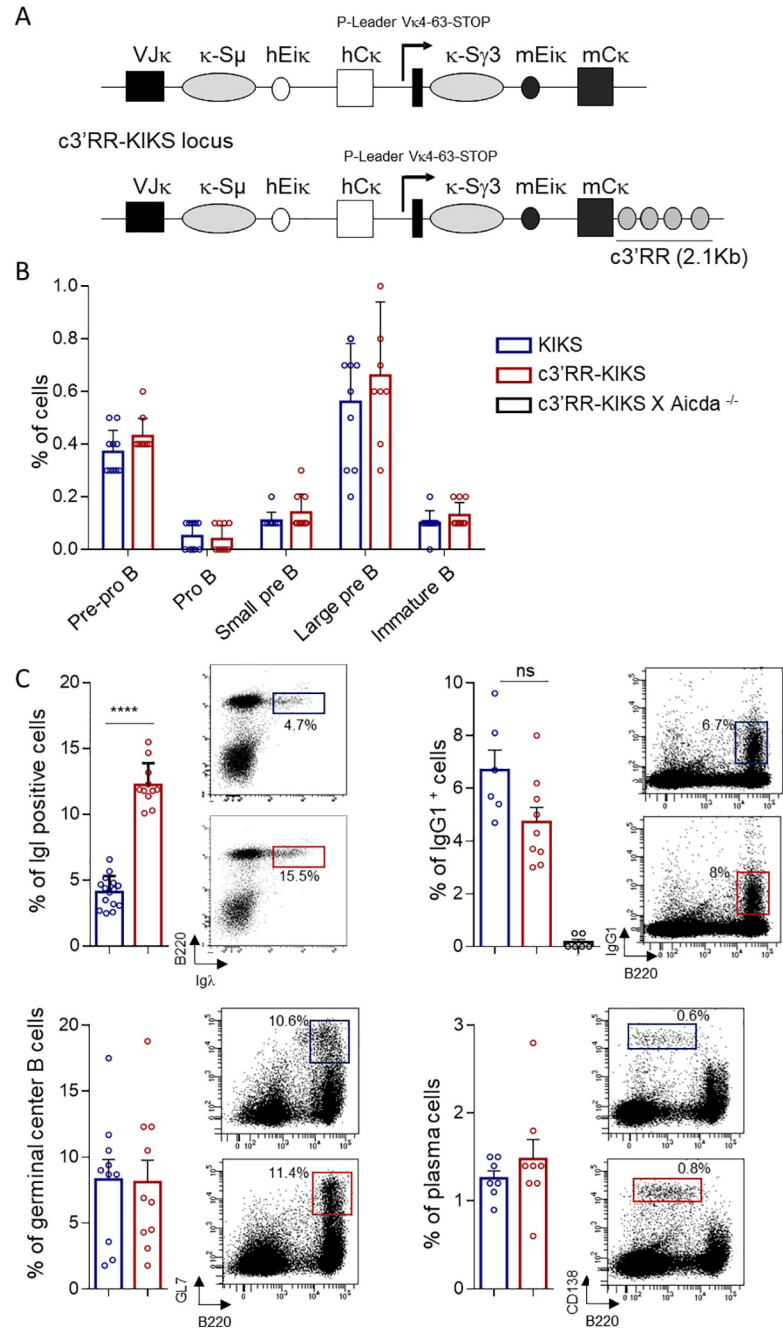
Fig 1. B-cell development. (A) Comparison between switchable Igκ loci. In *c3'RR-KIKS* mice, a *c3'RR* was inserted downstream of the locus. (B) Flow cytometry analysis of B-cell compartments in bone marrow. Percentages are given with mean+/- SEM as determined among total gated bone marrow lymphocytes. Data are representative of 10 animals of each genotype (left panel). (C) Flow cytometry analysis with representative dot plots, in spleen after SRBC immunization (D8), of switched B-cells (B220^{+}/IgG1^{+}), GC B-cells (B220^{+}/GL7^{+}) and plasma cells (B220^{low}/CD138^{+}) and mλ positive cells in non-immunized spleen. For switched B-cells, GC B cells and mλ the % are expressed on B220^{+} cells, and the % of plasma cells are expressed on total lymphocytes. Data are representative of 6 to 10 animals of each genotype. Percentages are given with mean+/- SEM. Mann-Whitney *U*-test for significance.

https://doi.org/10.1371/journal.pgen.1009288.g001

c3'RR-KIKS mice and *KIKS* mice, showing normal distribution of bone marrow pre-pro B, proB, large preB, small preB and immature B-cell populations (Figs 1B and S2). We only noticed an occasional increase of Ig lambda usage (Igλ) in some *c3'RR-KIKS* compared to *KIKS* mice, suggesting that LC rearrangements might even be accelerated by the knocked-in *IgH* elements, with Igλ then more frequently superseding the early rearranged *Igκ*. Late B-cell development also occurred normally, with no differences either regarding classical *IgH* locus CSR (IgG1$^+$ cells in spleen), nor the accumulation of germinal center (GC) B-cells and plasma cells (Fig 1C).

The IgH 3' super-enhancer cassette increases in vivo and in vitro ectopic κ-CSR in c3'RR-KIKS mice

The reporter system included in the *KIKS* and *c3'RR-KIKS* loci was designed in order to monitor κ-CSR loci as a switch from expression of human κ (hCκ) to mouse κ-LC (mCκ) (Figs 1A and S1). *In vivo*, both *KIKS* and *c3'RR-KIKS* mice developed small numbers of "κ-switched" mCκ-expressing B-cells in spleen. We quantified IgH-switched B cells in spleens from non-immunized and SRBC-immunized mice by quantifying B220$^+$/IgM$^-$ cells in which IgG1-switched B cells represented a majority of IgH-switched B cells (Figs 2A and S3A). We first verified that spleen resting B-cells don't not express mCκ (S3B Fig). In nonimmunized spleens, where IgH-switched (B220$^+$, IgM$^-$) B-cells were only present in low numbers in both models (Fig 2A left panel), κ-CSR was detectable in low amounts and significantly increased under the influence of the *c3'RR* (0.7% in *c3'RR-KIKS vs* 0.28% in *KIKS*, *p = 0.0027*) (Fig 2A right panel and S2 Table). After SRBC immunization (boosting classical IgH-CSR in spleens), κ-CSR was also boosted in both models but the trend towards a higher level in *c3'RR-KIKS* mice did not reach statistical significance by comparison to that in *KIKS* mice (Fig 2A right panel and S2 Table). Peyer's patches represent a chronically inflamed lymphoid tissue, where classical IgH-CSR was higher than in spleens in both models (Fig 2B left panel). κ-CSR was also increased in Peyer's patches when considering total B-cells (again with a trend to higher κ-CSR in *c3'RR-KIKS vs KIKS* mice but not reaching significance at *p = 0.08*) (Fig 2B middle panel and S2 Table). Gated GC B-cells from Peyer's patches (*i.e.* activated GL7$^+$ B-cells), showed the clearest difference between both models when focusing on cells where CSR was ongoing, then revealing a significant increase driven by the *c3'RR* (3.2% *vs* 1.5% mCκ$^+$ cells, respectively in *c3'RR-KIKS* and *KIKS* mice, p = 0.003) (Fig 2B right panel and S2 Table). The mCκ$^+$ cells were detected only in cells that have switched at IgH locus. In both the KIKS and the c3'RR-KIKS mice, we found an almost undetectable level of κCSR (below 0.1%) when the analysis was focused on cells with an unswitched IgH locus (gated as IgM+) (S3C Fig). Although κ-CSR then remained 10 to 15 fold below the parallel IgH-CSR, this confirmed that it could be positively stimulated by integrating an *IgH* super-enhancer cassette into the modified *Igκ* locus. AID-dependence of the κ-CSR process was also confirmed by its abrogation in AID-deficient *c3'RR-KIKS* mice (Fig 2A and 2B). This increased number of mouse Igκ$^+$ B-cells at the BCR expression level also translated into a change in amounts of secreted Ig in sera, with secreted mouse κ-LCs significantly increased in both non-immunized (18.8μg/mL *vs* 6.1μg/mL, p = 0.0002) and SRBC-immunized (68μg/mL *vs* 27.6μg/mL, p = 0.016) *c3'RR-KIKS vs KIKS* mice (Fig 2C). We next monitored κ-CSR onset *in vitro* after LPS or LPS/IL4 stimulation. *In vitro* κ-CSR occurred at very low levels but, as *in vivo*, we observed a significant increase (p = 0.033 and p = 0.028 for LPS and LPS/IL4 stimulation, respectively) in mCκ$^+$ cells in *c3'RR-KIKS* mice by flow cytometry (Fig 3A and 3B and S2 Table) confirming the role of the c3'RR in κ-CSR regulation.
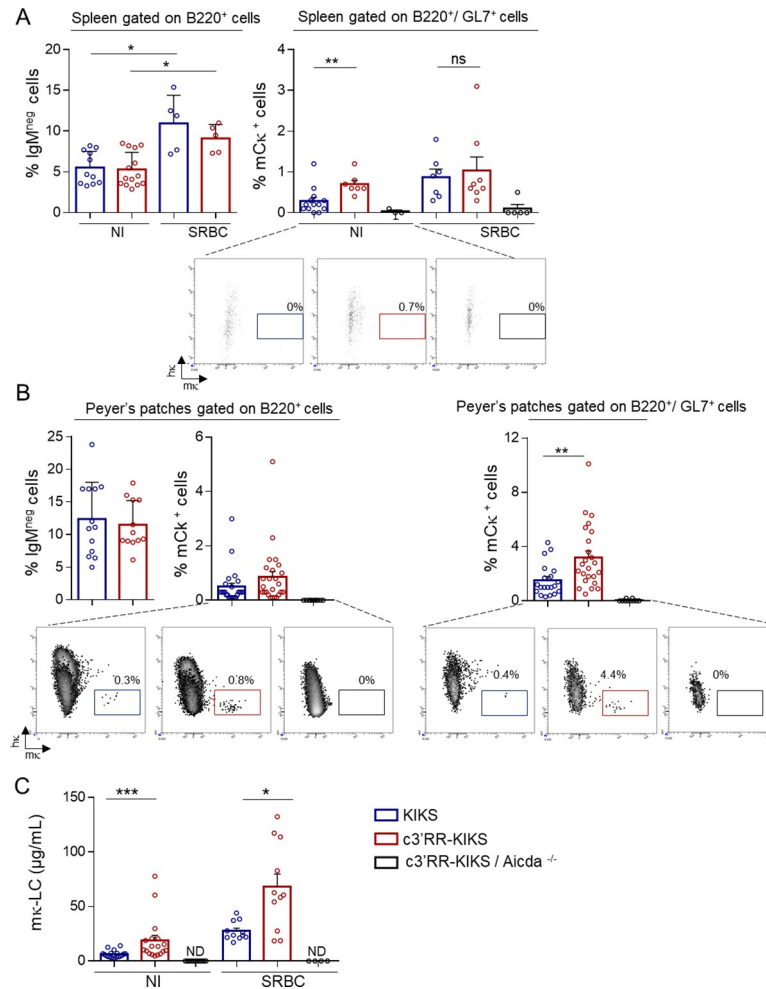
Fig 2. 3'RR core enhancers ectopically promote CSR *in vivo*. (A) Left: Evaluation of the amount of cells switching at the *IgH* locus (B220[+], IgM^{neg} cells) in spleens from NI or SRBC immunized mutant mice (day 8) Right: Comparison of κ-CSR efficiency as evaluated by counting mCκ[+] spleen B-cells (gated on B220[+]/GL7^{+} cells) by flow cytometry, in spleens from non-immunized (NI) or SRBC immunized (day 8) mice from *KIKS*, *c3'RR-KIKS* and *c3'RR-KIKS / Aicda^{-/-}* mice. Percentages +/- SEM are representative of 5 to 13 animals of each genotype (B) Left: Evaluation of the amount of cells switching at the *IgH* locus (B220[+], IgM^{neg} cells) in Peyer's patches from *KIKS*, *c3'RR-KIKS* mice. Middle and right: Comparison of κ-CSR efficiency as evaluated by counting mCκ[+] spleen B-cells either gated on B220 positive cells (*middle*) or on B220[+]/GL7[+](*right*) by flow cytometry, in Peyer's patches from *KIKS*, *c3'RR-KIKS* and *c3'RR-KIKS / Aicda^{-/-}* mice. Percentages +/- SEM are representative of 10 to 25 animals of each genotype. (C) ELISA quantification of serum mκ-LC in NI and SRBC-immunized mice (Day 8). Percentages +/- SEM are representative of 11 to 19 animals of each genotype.

Transcription and hypermutation of the knocked-in S regions prior to κ-CSR

AID targeting requires transcription for both SHM and CSR, and we thus assessed the amount of κ-S region primary transcripts in *KIKS* and *c3'RR-KIKS* Peyer's patches (Fig 4A). Both the κ-Sμ (p<0.0001) and κ-Sγ3 (p = 0.0007) regions proved significantly more transcribed in *c3'RR-KIKS* mice (Fig 4B and S3 Table). As expected upon transcription of a locus that is naturally accessible to AID and before any κ-CSR event, local hypermutation was clearly detectable within unrearranged κ-S regions and within the *Jκ5* 3' flanking intron from Peyer's patch GC B-cells. For un-switched κ-*Sμ*, we analyzed 570 bp downstream of *Jκ5*, (*i.e.* 220 bp from the 3'
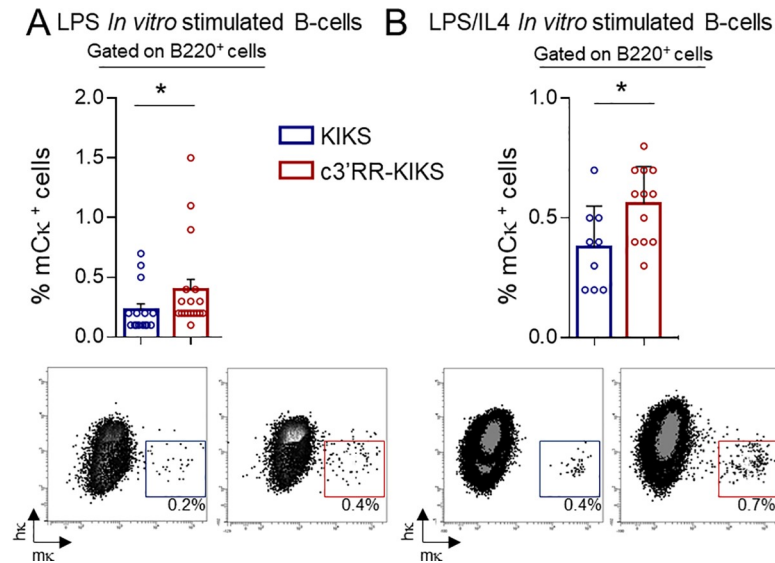
Fig 3. 3'RR core enhancers ectopically promote CSR *in vitro*. (A) Comparison of κ-CSR efficiency as evaluated by counting LPS *in vitro* stimulated mCκ+ spleen B-cells (gated on B220+ cells) by flow cytometry from *KIKS* and *c3'RR-KIKS* mice.(B) as in (A) for LPS/IL4 *in vitro* stimulation. Percentages are given with mean+/- SEM. Mann-Whitney test for significance.

Jκ5 flanking intron and 350 bp from the inserted κ-*Sμ*). We also analyzed the first 200 bp of un-switched κ-*Sγ3* (Fig 4A). To correct the substitution frequency at each nucleotide position along the sequenced region we used the DeMinEr tool [22], which uses deep sequencing data from mutated (*KIKS* and *c3'RR-KIKS*) and unmutated samples (*c3'RR-KIKS X Aicda* [-/-]). Using NGS, mutation frequencies in the [3'*Jκ5* intron—κ-*Sμ*] region were scored with reference to the *Jκ* rearrangement status (*Jκ1* or *Jκ5*). Confirming previous analyzes in *KIKS* mice [20], a high mutation rate at long distances from the promoter was observed throughout the [3'*Jκ5* intron—κ-*Sμ*] region (Fig 4C and S4 Table). In *c3'RR-KIKS* mice, this mutation rate tended to be higher than in *KIKS* mice (4.6 mut/kb *vs* 3.1 mut/kb for *Jκ1* rearrangement and 12.1 mut/kb *vs* 9.6 mut/kb for *Jκ5* rearrangement) (Fig 4C). By contrast, the mutation load of the acceptor κ-*Sγ3* region did not significantly differ (Fig 4C right panel and S4 Table). Thus, inclusion of the *c3'RR* globally increased transcription of κ-S regions and increased SHM around the donor κ-Sμ region in unswitched cells. This confirms the *Igκ* locus as a privileged non-*IgH* location strongly exposing knocked-in S regions to AID, but still with possible modulation by the inclusion of an additional Ig enhancer. Since the increased κ-CSR competence brought by the surrogate *c3'RR* seems to correlate with both higher transcription and with equivalent or higher AID-induced SHM prior to κ-CSR (in *c3'RR-KIKS vs KIKS* mice), we next wanted to precisely compare the structures of recombined switch junctions in both models.

Molecular analysis of SHM within switch junctions

We analyzed the total mutation load in hybrid κ-S regions from B220+/mk+ cells from Peyers' patches by specifically amplifying the rearranged κ-Sμ/κ-Sγ3 regions by nested PCR (Fig 5A). As expected, in both Igκ knock-in configurations, this rate was globally higher for rearranged κ-Sμ/Sγ3 junctions than for unrearranged κ-S regions (Figs 5B and 4C). However, the respective ranking of both models for SHM occurrence then appeared unexpectedly inversed: less SHM was present in rearranged κ-S sequences from *c3'RR-KIKS* (12.5 mut/kb: 93 mutations/
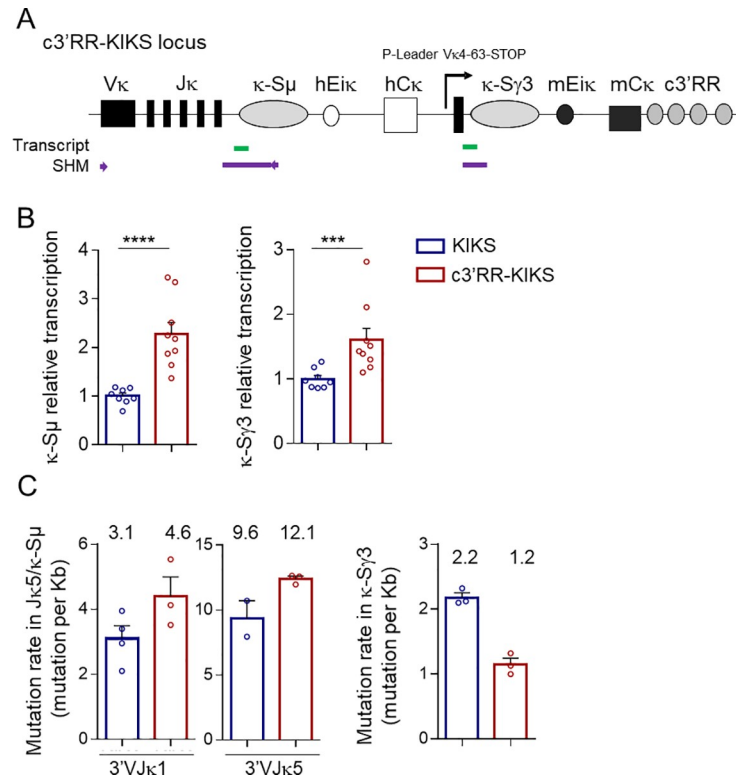
Fig 4. 3'RR core enhancers enhance transcription and SHM. (A) c3'RR-KIKS locus with the location of regions (thick lines) that were tested either for transcription (green) or for SHM (purple). Arrows represent primers used for SHM PCR amplification. (B) Relative κ-Sμ and κ-Sγ3 region transcripts analyzed in Peyer's patch GC B-cells (GC) (n = 8 to 9 mice) from *KIKS* and *c3'RR-KIKS* mice. (C) Mutation rate in the [3'*Jκ5* intron—κ-*Sμ*] region according to the Jκ rearrangement (Jκ1 or Jκ5) (left and middle panels) and mutation rates in the κ-Sγ3 region (right panel) (n = 2 to 4 individual mice) in GC B cells from KIKS, c3'RR-KIKS and *c3'RR-KIKS / Aicda^{-/-}* mice. The mutation frequency (mutations per Kb) is indicated over the bar graphs. Data are mean ± SEM, Mann-Whitney test for significance.

7414 pb analyzed) than from *KIKS* B-cells (15.6 mut/kb: 1140 mutations/92472 pb analyzed) (p = 0.029) (Fig 5B). This suggests that in the *Igκ* locus, presence of the c3'RR facilitates / accelerates either the occurrence of DSBs or their repair through synapsis of paired targets. The *3'RR* thus impacts the outcome of AID-initiated lesions and locally tends to increase the recombination *vs* mutation ratio.

To precisely analyze κ-CSR events in our models, we amplified CSR junctions using LAM-HTGTS [23]. By reference to a bait chosen upstream of a given DNA double-stranded break (DSB), this unbiased strategy detects junctions to "preys" located genome-wide. The κ-CSR events were captured by a 3'Jκ5 intron bait (κ-Sμ bait) chosen upstream of the knock-in donor κ-Sμ (Fig 5A). In order to identify and score the sequences joined to baits, non-redundant junctions were then analyzed using the algorithm published by Alt and colleagues [23].

Baits were found to be associated in *cis* or *trans* with sequences from either the *Igκ* KI (*cis* κ- CSR) or the endogenous *IgH* locus (*trans* κ-CSR). Analyzing the partners joined to the 3'Jκ5 intron bait (thereafter "κ-Sμ bait") in both κ-CSR models, showed that the predominant type of recombination was local intra-Sμ deletion (ISD), whether the analysis concerned LPS-activated splenocytes or Peyer's patches (Fig 5C and 5D). Alternatively, junctions to a distant κ-S region truly featuring *cis* κ-CSR also occurred, and were more frequent in the *c3'RR-KIKS* than in *KIKS* samples. This difference was dramatic when assessing ongoing *cis* κ-CSR *in vitro* by stimulating naive splenocytes, where Sμ-Sγ3 κ-CSR represented about 2.5% of all "Ig
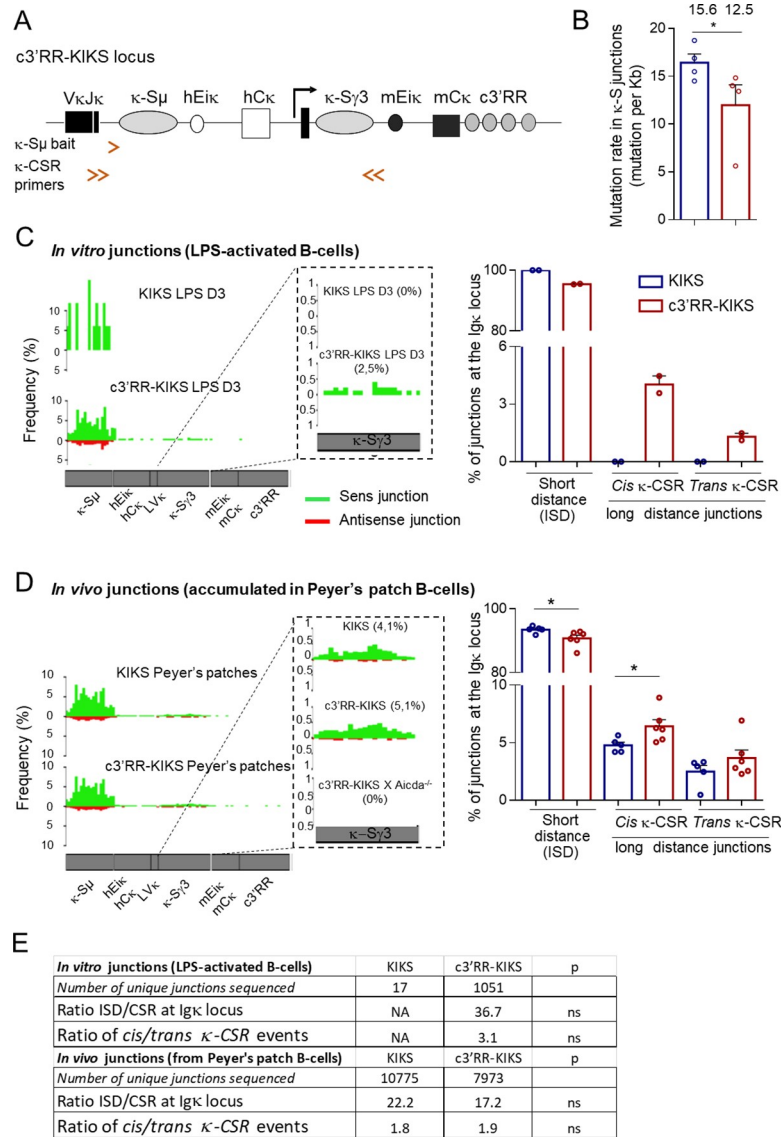
Fig 5. κ-CSR junction analysis. (A) *c3'RR-KIKS* locus with the location of κ-Sμ bait used for LAM-HTGS and primers used for κ-CSR amplification by nested PCR (double arrows). (B) Mutation rates (mutations per kb) in recombined κ-Sμ/Sγ3 junctions are indicated over the bar graphs. κ-Sμ/Sγ3 junctions were obtained by nested-PCR from mCk+ cells from Peyer's patches (n = 4 for each genotype). SHM was analyzed using CSReport. (C) κ-CSR junctions identified by LAM-HTGTS from *in vitro* activated B-cells. Map of junctions identified by LAM-HTGTS along the KI locus (left). Bar graphs (right) with percentages of ISD, *cis* κ-CSR internal to the Igκ locus and *trans* κ-CSR (Igκ-IgH) events obtained by LAM-HTGTS. Unique junctional sequences (each corresponding to multiple identical reads) were analyzed; the percentage of "Ig recombination events" (*i.e.* junctions of the bait with Ig sequences, either *Igκ* KI or *IgH*) is given. (D) κ-CSR junctions identified by LAM-HTGTS *in vivo* from Peyer's patch B-cells. (E) Table indicating the number of junctional sequences analyzed, ratio of *cis / trans* events, ratio of ISD/CSR within the endogenous *IgH* locus, and ratio of *cis/trans* events.

https://doi.org/10.1371/journal.pgen.1009288.g005

recombination events" in *c3'RR-KIKS*, while remaining undetectable in *KIKS* cells (Fig 5C and 5D).

LAM-HTGTS also confirmed that *in vivo*, Sμ-Sγ3 κ-CSR within the *Igκ* locus was more frequent in *c3'RR-KIKS* than in *KIKS* mice. Although less striking than *in vitro*, the difference was still significant (5.1% *vs* 4.1% of all "Ig recombination events", p = 0.04) (Fig 5D).

Globally, the "ISD / κ-CSR" ratio (*i.e.* the proportion of local *vs* distant recombination) thus decreased in all conditions where *c3'RR* was included, and this effect was most significantly visible when activating naive cells *in vitro* and thus estimating *de novo* recombination (Fig 5E).

Altogether, these data were in agreement with flow cytometry analyses and also confirmed AID-dependence of the process since very few junctions to the bait were found in control *c3'RR-KIKS* / *Aicda*^{-/-} mice and none of them featured CSR (Fig 5D). In addition to *cis* κ-CSR junctions internal to the *Igκ* locus (κ-Sμ to κ-Sγ3), some *trans* κ-CSR recombination events joined the κ-Sμ to acceptor S regions (Sγ3, Sγ1, Sγ2b, Sγ2a, Sε, Sα) from the endogenous *IgH* locus (Fig 5C and 5D). T*rans IgH*-CSR is known to abundantly occur between both *IgH* alleles and can account for up to 15% of all normal *IgH* CSR events [27, 28]. This figure appears even higher for κ-CSR, since more than one-third of κ-CSR junctions implicated an acceptor S region from the *IgH* locus (Fig 5C and 5D), corresponding to a *trans* κ-CSR rearrangement. This *trans/cis* κ-CSR ratio did not significantly differ in both κ-CSR models and the global stimulatory effect of the c3'RR on distant κ-CSR manifested equivalently for the prevalent *cis* junctions and the alternative *trans* pathway (Fig 5E).

Regarding repair of κ-CSR, junctions analyzed after sequencing of nested-PCR products from mCκ^{+} cells from Peyer's patches showed predominant blunt junctions, similar to classical CSR in *wt* mice. There was thus no apparent bias in the usage of either NHEJ or microhomology-mediated repair (Fig 6A). We consistently analyzed breakpoint distribution throughout the κ-S regions and found that breaks occurred as expected around AID hot spots. No difference in breakpoint dispersion in the κ-S region occurred between the two models (Fig 6B) suggesting that c3'RR does not impact the position break but rather the outcome of the breaks.

Globally considering κ-CSR (either in *cis* or *trans*), the present data indicate that integration of the *c3'RR* into the locus facilitated long distance synapses between AID-targeted DNA regions, rather than local deletions restricted to κ-Sμ. The *c3'RR* also tended to increase SHM of unrearranged κ-S regions (the level of which was higher in both models than observed in parallel for the *IgH* locus S regions) (Fig 4C). Strikingly, the *c3'RR*, however, facilitated the occurrence of junctions instead of less parallel local SHM. This change in the SHM/CSR ratio is in agreement with the observation made when comparing κ-CSR and parallel IgH-CSR, which can occur with minimal associated local SHM. In controls, we measured CSR at the endogenous *IgH* locus [23] and as expected, *IgH*-CSR was unaltered by the *Igκ* knock-in (with a majority of Sμ-Sα junctions in Peyer's patches) (Fig 7A and 7B); the SHM load of these S-S junctions could thus be evaluated and was found to be 2 to 3 fold lower in the *IgH* locus (where the complete *3'RR* likely optimized the CSR/SHM ratio) compared to the *Igκ* locus (Fig 7C and S5 Table).

CSR and SHM are thoroughly intermingled processes in physiology and there are few situations where they appear uncoupled, as observed in patients with immune deficiencies and N-terminal mutations of AID, affecting SHM while preserving CSR [24, 29]. By contrast, normal *IgH* CSR usually associates with some local SHM focused on WRCY motifs even after short *in vitro* stimulation of B-cells. This minimal SHM level has long been considered as only supporting CSR in *in vitro* conditions [30]. AID targeting to S regions strongly relies on their structure, abundance of WRCY motifs, potential binding of these motifs by 14-3-3, G4-richness and ability to promote the formation of R-loops when transcribed [16, 31, 32]. This favors RNA Polymerase II stalling in association with Spt5 and recruits AID together with the exosome which locally degrades S region transcripts and exposes both strands of R-loops to cytidine deamination [33, 34]. The *3'RR* promotes DNA looping within the *IgH* locus. Such loops facilitate transcription on one hand and specific interaction of the stalled polymerase II with Spt5, AID and other cofactors, and, on the other hand, ligation of paired S regions [16, 19]. By analogy in our κ-CSR model, it seems likely that the *c3'RR* can promote an *Igκ* locus
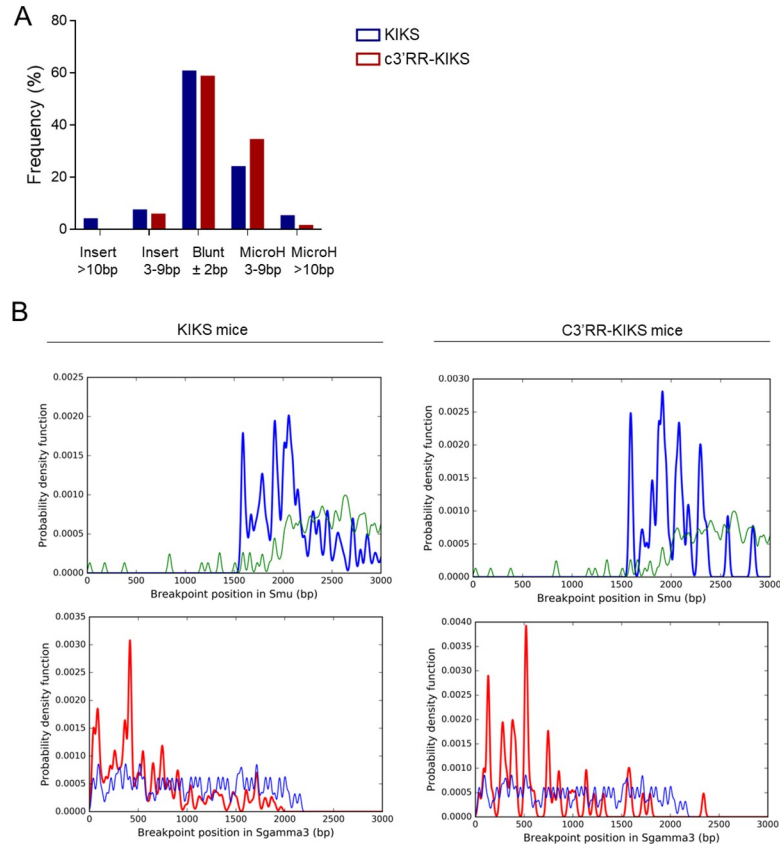
Fig 6. Structures and breakpoints distribution of κ-CSR junctions. (A) Structures of κ-*CSR* junctions obtained by nested-PCR from mκ+ cells from Peyer's patches and analyzed using CSReport. (B) Breakpoint distribution of κ-*CSR* junctions obtained by nested-PCR from mκ+ cells from Peyer's patches and analyzed using CSReport. Thick and thin lines represented breakpoints and AID motifs respectively.

https://doi.org/10.1371/journal.pgen.1009288.g006

conformation that is either more susceptible to single strand lesions and SHM or forms alternative loops that favor the occurrence of DSBs, terminates SHM and supports the synapsis of S regions prior to their ligation (as during classical CSR at the *IgH* locus).

As a conclusion, using a genetically engineered *Igκ* locus as a CSR substrate, we observed that inclusion of a surrogate *3'RR* promoted CSR recombination in multiple aspects. It increased both the balance of CSR *vs* SHM on CSR-targeted S regions and the balance of recombination with distant partners *vs* local intra-Sμ deletion for the knocked-in donor Sμ region. The increased frequency of distant events primarily concerned *cis-CSR* within the modified *Igκ* locus, but also equally affected *trans-CSR* joining the *Igκ / IgH* loci.

Altogether, this study shows that the *IgH 3'RR* can instrumentally promote the transformation of AID-initiated lesions into CSR breaks rather than SHM and promote junctions with distant CSR targets rather than local deletion.

This study thus directly confirms those roles of the *3'RR* that have been previously postulated indirectly after analyzing *3'RR*-deficient mice (which show anomalies of both *IgH cis*- and *trans*-CSR). While repair pathways of junctions did not vary between control loci or loci integrating the *3'RR*, our data are consistent with the notion that the *3'RR* promotes synapsis between distant CSR targets prior to recombination. This fits with a model where the *3'RR* would participate in the assembly of a CSR factory, bringing both the loops formed in *cis* on a targeted locus, and potential other legitimate targets from other chromosomes (usually the
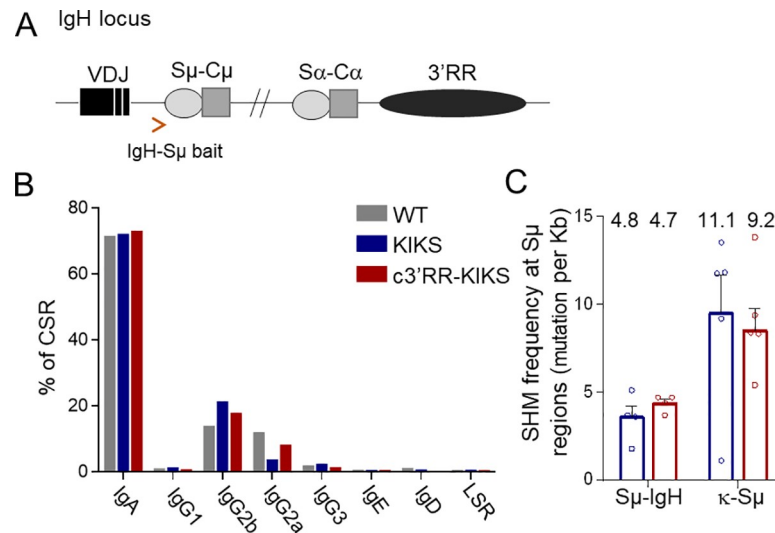
Fig 7. c3'RR at KI locus does not affect CSR and SHM at *IgH* locus. (A) *IgH* locus with the location of IgH-Sμ bait used for LAM-HTGS. () Percentage of switched *IgH* isotypes in Peyer's patch B-cells from *KIKS* (n = 4), *c3'RR-KIKS* (n = 3) and *wt* (n = 3) mice obtained by LAM-HTGTS. (C) Mutation rate (mutation per kb) in IgH-*Sμ* (n = 4) and κ-*Sμ* (n = 5) after CSR recombination obtained by LAM-HTGTS from Peyer's patches.

other *IgH* allele but also here a knocked-in *Igκ KIKS* allele). This schema must thus accommodate not only the "loop model" [19] but also the data concurring to demonstrate the efficient interactions of S regions even when located on different chromosomes [27, 28, 35, 36].

That κ-CSR remains about 10 to 15-fold less frequent than *IgH* CSR in the *c3'RR-KIKS* locus is expected since the 3' IgH super-enhancer stands as an extensive region with multiple functional modules in the *IgH* locus, which can hardly be replaced by a *c3'RR* cassette restricted to core enhancers. Notably, we previously demonstrated that the intervening sequences located in-between core enhancers architecturally contribute to the CSR-boosting effect exerted by the super-enhancer [13]. Dealing with chromosomal loops, the *IgH* locus context has by itself accumulated multiple elements favoring the occurrence of CSR loops, and the normal *IgH 3'RR* is notably followed by multiple CTCF binding elements which might ideally anchor the 3'RR within a CSR factory at the basis of a CSR loop [37]. Alt and coll thus recently proposed that CTCF and cohesin-bound elements dynamically support "loop extrusion" and enable the *3'RR* to promote secondary loops for S region synapsis and cleavage, underlining the importance of the long range locus topology and chromosomal context [38]. In an attempt to identify the necessary constituents of a functional switching domain, our comparison of two artificial Ig loci with identical structures, AID accessibility, G4-density and location of S regions within introns, but only differing by inclusion of a *c3'RR*, confirms the instrumental contribution of the *3'RR* enhancers to CSR competence beyond SHM.

Supporting information

S1 Fig. The *c3'RR-KIKS* construct was inserted into the Igκ locus by homologous recombination (not to scale). The inserted cassette includes the core Sμ, followed by the hEiκ enhancer, constant hCκ exon from the human Igκ locus and then the core *Sγ3* and *c3'RR*. A *Vκ* promoter and mutated leader exon provides transcription and splicing of *Sγ3*. The downstream floxed NeoR gene was removed by Cre-deletion to generate the germline *c3'RR-KIKS* locus. *c3'RR-KIKS* κ-CSR events join *S* regions, then excising *hCk* and yielding Ig with murine

Ck.
(TIF)

S2 Fig. Gating strategy to study B cell development in the bone marrow.
(TIF)

S3 Fig. A. Percentage of IgG1+ cells in spleens from NI or SRBC immunized mice (day 8) (KIKS, c3'RR-KIKS and c3'RR-KIKS / Aicda-/- mice). B. Representative dot plots of mκ and hκ staining in CD43 negative splenic B-cells. C Comparison of κ-CSR efficiency as evaluated by counting mCκ+ spleen B-cells (gated on B220+/IgM+ cells) by flow cytometry, in spleens from non-immunized (NI) or SRBC immunized (day 8) mice and from Peyers' patches from KIKS, c3'RR-KIKS and c3'RR-KIKS / Aicda-/- mice. Percentages +/- SEM.
(TIF)

S1 Table. Antibodies used in this study.
(XLSX)

S2 Table. Each individual experiment of κ-CSR efficiency as evaluated by counting mCκ$^+$ spleen B-cells (gated on B220$^+$/GL7$^+$ cells) and by B220 positive cells or on B220$^+$/GL7$^+$ in Peyer's patches from *KIKS, c3'RR-KIKS* and *c3'RR-KIKS / Aicda$^{-/-}$* mice. B: Each individual experiment of κ-CSR efficiency as evaluated by counting mCκ$^+$ in *in vitro* stimulated (LPS) B-cells (gated on B220$^+$).
(XLSX)

S3 Table. Cycle numbers of the qPCR reaction obtained for GAPDH, κ-Sμ and κ-Sγ3 region transcripts analyzed in Peyer's patch GC B-cells (GC) from *KIKS* and *c3'RR-KIKS* mice.
(XLSX)

S4 Table. Total number of mutations, total number of bp analyzed and mutation rates for [3'*Jκ5* intron—κ-*Sμ*] and κ-Sγ3 regions in *KIKS* and *c3'RR-KIKS* mice.
(XLSX)

S5 Table. Total number of mutations, total number of bp analyzed and mutation rates for *IgH*-Sμ or κ-Sμ regions in *KIKS* and *c3'RR-KIKS* mice.
(XLSX)

Acknowledgments

Author Contributions

Conceptualization: Christophe Sirac, Michel Cogné.

Funding acquisition: Christophe Sirac, Michel Cogné.

Investigation: Sandrine Le Noir, Amélie Bonaud, Bastien Hervé, Audrey Baylet, François Boyer, Sandrine Lecardeur, Zeliha Oruc, Michel Cogné.

Methodology: Sandrine Le Noir, Amélie Bonaud, Christophe Sirac, Michel Cogné.

Writing – original draft: Sandrine Le Noir.

Writing – review & editing: Sandrine Le Noir, Amélie Bonaud, Christophe Sirac, Michel Cogné.

References

1. Conticello SG, Thomas CJF, Petersen-Mahrt SK, Neuberger MS. Evolution of the AID/APOBEC family of polynucleotide (deoxy)cytidine deaminases. Mol Biol Evol. 2005; 22: 367–377. https://doi.org/10.1093/molbev/msi026 PMID: 15496550

2. Boehm T, McCurley N, Sutoh Y, Schorpp M, Kasahara M, Cooper MD. VLR-based adaptive immunity. Annu Rev Immunol. 2012; 30: 203–220. https://doi.org/10.1146/annurev-immunol-020711-075038 PMID: 22224775

3. Xu Z, Zan H, Pone EJ, Mai T, Casali P. Immunoglobulin class-switch DNA recombination: induction, targeting and beyond. Nat Rev Immunol. 2012; 12: 517–531. https://doi.org/10.1038/nri3216 PMID: 22728528

4. Cogné M, Lansford R, Bottaro A, Zhang J, Gorman J, Young F, et al. A class switch control region at the 3' end of the immunoglobulin heavy chain locus. Cell. 1994; 77: 737–747. https://doi.org/10.1016/0092-8674(94)90057-4 PMID: 8205622

5. Pinaud E, Khamlichi AA, Le Morvan C, Drouet M, Nalesso V, Le Bert M, et al. Localization of the 3′ IgH Locus Elements that Effect Long-Distance Regulation of Class Switch Recombination. Immunity. 2001; 15: 187–199. https://doi.org/10.1016/s1074-7613(01)00181-9 PMID: 11520455

6. Vincent-Fabert C, Fiancette R, Pinaud E, Truffinet V, Cogné N, Cogné M, et al. Genomic deletion of the whole IgH 3' regulatory region (hs3a, hs1,2, hs3b, and hs4) dramatically affects class switch recombination and Ig secretion to all isotypes. Blood. 2010; 116: 1895–1898. https://doi.org/10.1182/blood-2010-01-264689 PMID: 20538806

7. Péron S, Laffleur B, Denis-Lagache N, Cook-Moreau J, Tinguely A, Delpy L, et al. AID-driven deletion causes immunoglobulin heavy chain locus suicide recombination in B cells. Science. 2012; 336: 931–934. https://doi.org/10.1126/science.1218692 PMID: 22539552

8. Chaudhuri J, Alt FW. Class-switch recombination: interplay of transcription, DNA deamination and DNA repair. Nat Rev Immunol. 2004; 4: 541–552. https://doi.org/10.1038/nri1395 PMID: 15229473

9. Saintamand A, Vincent-Fabert C, Garot A, Rouaud P, Oruc Z, Magnone V, et al. Deciphering the importance of the palindromic architecture of the immunoglobulin heavy-chain 3' regulatory region. Nat Commun. 2016; 7: 10730. https://doi.org/10.1038/ncomms10730 PMID: 26883548

10. Honjo T, Kinoshita K, Muramatsu M. Molecular mechanism of class switch recombination: linkage with somatic hypermutation. Annu Rev Immunol. 2002; 20: 165–196. https://doi.org/10.1146/annurev.immunol.20.090501.112049 PMID: 11861601

11. Pefanis E, Wang J, Rothschild G, Lim J, Kazadi D, Sun J, et al. RNA exosome-regulated long non-coding RNA transcription controls super-enhancer activity. Cell. 2015; 161: 774–789. https://doi.org/10.1016/j.cell.2015.04.034 PMID: 25957685

12. Chauveau C, Cogné M. Palindromic structure of the IgH 3'locus control region. Nat Genet. 1996; 14: 15–16. https://doi.org/10.1038/ng0996-15 PMID: 8782813

13. Le Noir S, Boyer F, Lecardeur S, Brousse M, Oruc Z, Cook-Moreau J, et al. Functional anatomy of the immunoglobulin heavy chain 3′ super-enhancer needs not only core enhancer elements but also their unique DNA context. Nucleic Acids Res. 2017; 45: 5829–5837. https://doi.org/10.1093/nar/gkx203 PMID: 28369649

14. Pinaud E, Marquet M, Fiancette R, Péron S, Vincent-Fabert C, Denizot Y, et al. The IgH locus 3' regulatory region: pulling the strings from behind. Adv Immunol. 2011; 110: 27–70. https://doi.org/10.1016/B978-0-12-387663-8.00002-8 PMID: 21762815

15. Saintamand A, Rouaud P, Saad F, Rios G, Cogné M, Denizot Y. Elucidation of IgH 3' region regulatory role during class switch recombination via germline deletion. Nat Commun. 2015; 6: 7084. https://doi.org/10.1038/ncomms8084 PMID: 25959683

16. Wang L, Wuerffel R, Feldman S, Khamlichi AA, Kenter AL. S region sequence, RNA polymerase II, and histone modifications create chromatin accessibility during class switch recombination. J Exp Med. 2009; 206: 1817–1830. https://doi.org/10.1084/jem.20081678 PMID: 19596805

17. Li G, White CA, Lam T, Pone EJ, Tran DC, Hayama KL, et al. Combinatorial H3K9acS10ph Histone Modification in IgH Locus S Regions Targets 14-3-3 Adaptors and AID to Specify Antibody Class-Switch DNA Recombination. Cell Rep. 2013; 5: 702–714. https://doi.org/10.1016/j.celrep.2013.09.031 PMID: 24209747

18. Jeevan-Raj BP, Robert I, Heyer V, Page A, Wang JH, Cammas F, et al. Epigenetic tethering of AID to the donor switch region during immunoglobulin class switch recombination. J Exp Med. 2011; 208: 1649–1660. https://doi.org/10.1084/jem.20110118 PMID: 21746811

19. Wuerffel R, Wang L, Grigera F, Manis J, Selsing E, Perlot T, et al. S-S Synapsis during Class Switch Recombination Is Promoted by Distantly Located Transcriptional Elements and Activation-Induced Deaminase. Immunity. 2007; 27: 711–722. https://doi.org/10.1016/j.immuni.2007.09.007 PMID: 17980632

20. Bonaud A, Lechouane F, Le Noir S, Monestier O, Cogné M, Sirac C. Efficient AID targeting of switch regions is not sufficient for optimal class switch recombination. Nat Commun. 2015; 6: 7613. https://doi.org/10.1038/ncomms8613 PMID: 26146363

21. Boyer F, Boutouil H, Dalloul I, Dalloul Z, Cook-Moreau J, Aldigier J-C, et al. CSReport: A New Computational Tool Designed for Automatic Analysis of Class Switch Recombination Junctions Sequenced by High-Throughput Sequencing. J Immunol Baltim Md 1950. 2017; 198: 4148–4155. https://doi.org/10.4049/jimmunol.1601924 PMID: 28416601

22. Martin OA, Garot A, Le Noir S, Aldigier J-C, Cogné M, Pinaud E, et al. Detecting Rare AID-Induced Mutations in B-Lineage Oncogenes from High-Throughput Sequencing Data Using the Detection of Minor Variants by Error Correction Method. J Immunol Baltim Md 1950. 2018; 201: 950–956. https://doi.org/10.4049/jimmunol.1800203 PMID: 29898966

23. Hu J, Meyers RM, Dong J, Panchakshari RA, Alt FW, Frock RL. Detecting DNA double-stranded breaks in mammalian genomes by linear amplification-mediated high-throughput genome-wide translocation sequencing. Nat Protoc. 2016; 11: 853–871. https://doi.org/10.1038/nprot.2016.043 PMID: 27031497

24. Dong J, Panchakshari RA, Zhang T, Zhang Y, Hu J, Volpi SA, et al. Orientation-specific joining of AID-initiated DNA breaks promotes antibody class switching. Nature. 2015; 525: 134–139. https://doi.org/10.1038/nature14970 PMID: 26308889

25. Frock RL, Hu J, Meyers RM, Ho Y-J, Kii E, Alt FW. Genome-wide detection of DNA double-stranded breaks induced by engineered nucleases. Nat Biotechnol. 2015; 33: 179–186. https://doi.org/10.1038/nbt.3101 PMID: 25503383

26. Gel B, Serra E. karyoploteR: an R/Bioconductor package to plot customizable genomes displaying arbitrary data. Bioinforma Oxf Engl. 2017; 33: 3088–3090. https://doi.org/10.1093/bioinformatics/btx346 PMID: 28575171

27. Laffleur B, Bardet SM, Garot A, Brousse M, Baylet A, Cogné M. Immunoglobulin genes undergo legitimate repair in human B cells not only after cis- but also frequent trans-class switch recombination. Genes Immun. 2014; 15: 341–346. https://doi.org/10.1038/gene.2014.25 PMID: 24848929

28. Reynaud S, Delpy L, Fleury L, Dougier H-L, Sirac C, Cogné M. Interallelic class switch recombination contributes significantly to class switching in mouse B cells. J Immunol Baltim Md 1950. 2005; 174: 6176–6183. https://doi.org/10.4049/jimmunol.174.10.6176 PMID: 15879114

29. Shinkura R, Ito S, Begum NA, Nagaoka H, Muramatsu M, Kinoshita K, et al. Separate domains of AID are required for somatic hypermutation and class-switch recombination. Nat Immunol. 2004; 5: 707–712. https://doi.org/10.1038/ni1086 PMID: 15195091

30. Yeap L-S, Hwang JK, Du Z, Meyers RM, Meng F-L, Jakubauskaitė A, et al. Sequence-Intrinsic Mechanisms that Target AID Mutational Outcomes on Antibody Genes. Cell. 2015; 163: 1124–1137. https://doi.org/10.1016/j.cell.2015.10.042 PMID: 26582132

31. Yu K, Chedin F, Hsieh C-L, Wilson TE, Lieber MR. R-loops at immunoglobulin class switch regions in the chromosomes of stimulated B cells. Nat Immunol. 2003; 4: 442–451. https://doi.org/10.1038/ni919 PMID: 12679812

32. Xu Z, Fulop Z, Wu G, Pone EJ, Zhang J, Mai T, et al. 14-3-3 adaptor proteins recruit AID to 5′-AGCT-3′–rich switch regions for class switch recombination. Nat Struct Mol Biol. 2010; 17: 1124–1135. https://doi.org/10.1038/nsmb.1884 PMID: 20729863

33. Chandra V, Bortnick A, Murre C. AID targeting: old mysteries and new challenges. Trends Immunol. 2015; 36: 527–535. https://doi.org/10.1016/j.it.2015.07.003 PMID: 26254147

34. Basu U, Meng F-L, Keim C, Grinstein V, Pefanis E, Eccleston J, et al. The RNA Exosome Targets the AID Cytidine Deaminase to Both Strands of Transcribed Duplex DNA Substrates. Cell. 2011; 144: 353–363. https://doi.org/10.1016/j.cell.2011.01.001 PMID: 21255825

35. Kingzette M, Spieker-Polet H, Yam PC, Zhai SK, Knight KL. Trans-chromosomal recombination within the Ig heavy chain switch region in B lymphocytes. Proc Natl Acad Sci U S A. 1998; 95: 11840–11845. https://doi.org/10.1073/pnas.95.20.11840 PMID: 9751752

36. Le Noir S, Laffleur B, Carrion C, Garot A, Lecardeur S, Pinaud E, et al. The IgH locus 3' cis-regulatory super-enhancer co-opts AID for allelic transvection. Oncotarget. 2017; 8: 12929–12940. https://doi.org/10.18632/oncotarget.14585 PMID: 28088785

37. Garrett FE, Emelyanov AV, Sepulveda MA, Flanagan P, Volpi S, Li F, et al. Chromatin architecture near a potential 3' end of the igh locus involves modular regulation of histone modifications during B-Cell development and in vivo occupancy at CTCF sites. Mol Cell Biol. 2005; 25: 1511–1525. https://doi.org/10.1128/MCB.25.4.1511-1525.2005 PMID: 15684400

38. Zhang X, Zhang Y, Ba Z, Kyritsis N, Casellas R, Alt FW. Fundamental roles of chromatin loop extrusion in antibody class switching. Nature. 2019. https://doi.org/10.1038/s41586-019-1723-0 PMID: 31666703